Valorization of granulated slag of Arcelor-Mittal (Algeria) in cationic dye adsorption from aqueous solution: column studies

Radia Mazouz, Naima Filali, Zhour Hattab and Kamel Guerfi

ABSTRACT

A continuous adsorption study in a fixed-bed column was carried out using granulated slag (GS) as an adsorbent for the removal of methylene blue (MB) from aqueous solution. The effects of various parameters, such as initial dye concentration, flow rate, bed depth, and pH were investigated. Obtained results confirmed that the breakthrough time and exhaustion time were dependent on these factors. The adsorption capacity of GS was calculated at the 50% breakthrough point for different conditions. The highest breakthrough capacity ($q_{,exp} = 0.296$ mg.g^{-1}) was obtained with a 15 cm bed height and a 2 mL.min^{-1} rate by using a 10 mg.L^{-1} initial MB concentration at pH 7.5. Bohart–Adams, Bed Depth Service Time (BDST), and Thomas models were applied to experimental data to determine the characteristic parameters of the column. The Thomas model was found suitable for the description of the whole breakthrough curve, while the Bohart–Adams model was only used to predict the initial part of the dynamic process. The data were in good agreement with the BDST model. Thus, the granulated slag can be used as an adsorbent in the treatment of wastewater. Desorption was carried out with a deionized water as the desorbing agent, and reuse study was investigated.

Key words | breakthrough curve, cationic dye, dynamic adsorption, fixed bed column, granulated slag

Radia Mazouz (corresponding author)
Naima Filali
Zhour Hattab
Kamel Guerfi
Laboratory of Water Treatment & Revalorization of Industrial Waste, (LWTRIW),
Badji Mokhtar University,
Annaba,
Algeria
E-mail: *jihen2002@hotmail.com*

NOMENCLATURE

C_0	Initial MB concentration (mg.L^{-1})
C_t	Effluent MB concentration (mg.L^{-1})
C_b	Breakthrough concentration (mg.L^{-1})
F	Linear velocity (cm.min^{-1})
K_a	Rate constant in BDST model (L.mg^{-1}.min^{-1})
K_{BA}	Kinetic constant of Bohart–Adams model (L.mg^{-1}.min^{-1})
K_{TH}	Kinetic constant of Thomas model (L.mg^{-1}.min^{-1})
N_0	Saturation concentration of Bohart–Adams model (mg.L^{-1})
N_0'	Adsorption capacity in BDST model (mg.L^{-1})
$q_{50\%}$	Breakthrough capacity (mg.g^{-1})
q	Adsorption capacity of Thomas model (mg.g^{-1})
Q	Flow rate (mL·min^{-1})
t	Effluent time (min)
t_b	Breakthrough time (min)
t_e	Exhaustion or saturation time (min)
W	Adsorbent mass (g)
Z	Bed height of column (cm)

doi: 10.2166/wrd.2015.049

INTRODUCTION

Wastewaters discharged from many industries related to textiles, paper, plastics, food, and cosmetics cause water pollution and serious problems to the environment (Pearce *et al.* 2003; Aksu 2005; Zulfikar & Setiyanto 2013; Milenova *et al.* 2014). Due to their ease of production and cost-effectiveness, synthetic dyes are preferred in the textile industry compared to natural dyes (Abdul Halim & Kar Mee 2011;

Kumar & Tamilarasan 2013). They have complex molecular structures, which make them more stable and difficult to biodegrade (Seshadri *et al.* 1994; Fewson 1998; Li *et al.* 2009). Therefore, wastewaters containing dyes are treated before being discharged into water bodies (Elkassimi *et al.* 1998) by using different conventional methods (Blackburn 2004; Sampedro *et al.* 2004; Crini 2006; Mustafa *et al.* 2008). The adsorption technique is widely used and recommended in the treatment of effluents due to its inexpensive nature and ease of use (Aksu 2005). Batch adsorption experiments are generally used for the treatment of small volumes of effluent. Instead, adsorption in a fixed bed column is more applicable due to its low operating cost and the ability of columns to adapt to versatile processes (Cheknane *et al.* 2012).

Recently, many works have been studied for the development of low-cost adsorbents for water treatment including natural materials, biosorbents, and waste materials from industry and agriculture (Crini 2006; Han *et al.* 2009; Atshan 2014). Granulated slag (GS) is an industrial by-product in the production of cast iron, which causes a disposal problem. It was converted into an effective adsorbent and used for the removal of organic/inorganic pollutants (Ramakrishna & Viraraghvan 1997; Dimitrova & Mehandgiev 1998; Kostura *et al.* 2005; Das *et al.* 2007; Zhou & Haynes 2010). The presence of CaO, SiO_2, and Al_2O_3 in granulated slag contributes to its good adsorbent properties.

The focus of this work is to investigate the possibility of using granulated slag as an adsorbent for the removal of methylene blue (MB) from aqueous solution in a fixed bed column. The effects of initial dye concentration, flow rate, and bed depth on the breakthrough characteristics of the adsorption system were determined. The obtained results were presented in term of breakthrough curves. Three models, namely Bohart–Adams, Bed Depth Service Time (BDST), and Thomas were employed to predict the breakthrough curves and to determine the characteristic parameters useful for column design.

MATERIALS AND METHODS

The GS is a byproduct from the manufacture of Arcelor-Mittal (Algeria) with a rate of 97% vitrification, but low water content (Ader 1981). The material was dried for 24 h in an oven at 105–110 °C. The chemical composition of GS was determined in the Arcelor-Mittal laboratory using Fluorescence X (TW16006 PHILIPS). X-ray spectra showed that the used slag has an amorphous structure (Arabi *et al.* 2012). Size distribution was measured using a laser granulometer (Malvern Master Sizer), and the diameter was between 50 and 80 μm. The specific surface area was determined by the Brunauer–Emmett–Teller (BET) method (Brunauer *et al.* 1938) using a Micromeritics ASAP 2010 apparatus, and was found to be equal to 2.42 $m^2.g^{-1}$.

The basic dye, methylene blue, is the most commonly used material for dying cotton, wood, and silk. It was chosen in this study because of its strong adsorption onto solids. The chemical structures with general data of the dye are represented in Table 1. Serial dilutions of the stock solution were made to obtain specific concentrations required for the adsorption study.

Kinetic models

In order to predict the breakthrough curves of the adsorption process in the fixed bed, and estimate the parameters necessary for the design of a large-scale fixed-bed adsorber, the Bohart–Adams, BDST, and Thomas models have been used.

The Bohart–Adams model (Bohart & Adams 1920)

This is based on the surface reaction theory, to describe the relationship between C_t/C_0 and t in a continuous system, and is applied to describe the initial part of the breakthrough

Table 1 | General data on methylene blue

Dye	Formula	Molecular weight ($g.mol^{-1}$)	Chemical structure	Wave length (nm)
Methylene blue	$C_{16}H_{18}ClN_3S$	319.5	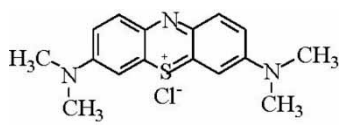	663

curve. The expression is given below (Ahmad & Hameed 2010):

$$\ln\left(\frac{C_t}{C_0}\right) = K_{AB}C_0(t) - \frac{K_{AB}N_0Z}{F} \quad (1)$$

The BDST model (Hutchins 1973)

The BDST model is used to predict the bed capacity by utilizing the different breakthrough values. The modified version of the equation used in this evaluation is given in Equation (2) (Janet *et al.* 2015):

$$t = \frac{N_0'}{C_0 F} Z - \frac{1}{K_a C_0}\ln\left(\frac{C_0}{C_b} - 1\right) \quad (2)$$

Thomas model (Thomas 1944)

This model is one of the most general and widely used models in the column performance theory. The linearized form of the model is given as (Han *et al.* 2009):

$$\ln\left(\frac{C_0}{C_t} - 1\right) = \frac{K_{TH}q\,W}{Q} - K_{TH}C_0t \quad (3)$$

Error analysis

A linear regressive method is used to compare the models using experimental data. To evaluate the validity of the models, there are different types of errors that indicate the appropriateness between the experimental and calculated adsorption capacity values. Therefore, the conformity of a model is better when the correlation coefficient is higher (Mathialagan & Viraraghavan 2002) and the error is lower (Tan *et al.* 2007). For this purpose, the experimental data were used to determine the error represented by the relative mathematical formula *SS* (Equation (4)) (Han *et al.* 2009):

$$SS = \frac{\sum\left[\left(C_t/c_0\right)_c - \left(C_t/C_0\right)_e\right]^2}{N} \quad (4)$$

where $\left(C_t/C_0\right)_c$ is the calculated ratio of MB concentrations according to dynamic models, and $\left(C_t/C_0\right)_e$ is the experimental ratio of MB concentrations. N is the number of the experimental point.

Experimental setup

Fixed bed column studies were performed at room temperature using a glass column of 1.1 cm internal diameter and 25 cm in length. A known quantity of adsorbent was then placed in the column to submit the desired bed height (5, 10 and 15 cm), keeping the same particle size (50–80 μm) obtained by sieving in order to maintain the same porosity for the adsorbent. A dye solution of known concentrations of 5, 10, and 15 mg.L^{-1} was pumped upward through the bed at different flow rates of 1, 2, and 3 mL.min^{-1} with a peristaltic pump (ISMATEC). Samples were collected at regular time intervals from the exit of the column for all the experiments. The concentration of the solution in the effluent was analyzed using a UV/VIS spectrophotometer (TECHCOMP) at 663 nm. Operation of the column was stopped when saturation was achieved. The experiments were performed in triplicate, and mean values were taken into account.

Analysis of column data

The operation of an adsorption column in dynamic mode can be determined by using the time to achieve the breakthrough and the shape of the breakthrough curve (Kanadasan *et al.* 2010). A typical breakthrough curve (Figure 1) is generally expressed by plotting C_t (effluent concentration) and C_t/C_0 (the normalized concentration, defined as the ratio of C_t to C_0 as a function of time (min) or treated volume V (mL).

The concentration at breakthrough point C_b, is chosen arbitrarily at a low value (in this study, when C_t reaches 10% of its initial value). When C_t approaches 90% of its initial concentration, the adsorbent is considered to be essentially exhausted (Faust & Aly 1987; Suksabye *et al.* 2008).

Breakthrough capacity $q_{50\%}$ (at 50% or $C_t/C_0 = 0.5$) expressed in mg of dye adsorbed per gram of

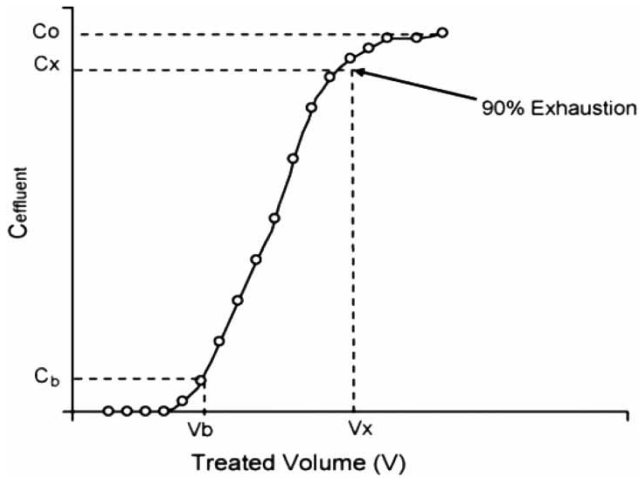

Figure 1 | Typical breakthrough curve (Al-Degs *et al.* 2009).

adsorbent was calculated by the following equation (Sadaf & Bhatti 2014):

$$\text{Breakthrough capacity } q_{50\%} = \frac{\text{breakthrough time } at\ 50\% * \text{flow rate} * \text{initial concentration}}{\text{adsorbent mass}} \quad (5)$$

RESULTS AND DISCUSSION

Characterization of the adsorbent

The results of the study of the chemical composition are shown in Table 2.

From the results, the GS seems to be constituted essentially of four elements: CaO, SiO_2, Al_2O_3, and MgO.

The effect of various parameters influencing adsorption was determined and the obtained results are presented in Table 3.

From these results, we can deduce the effects as follows.

Effect of bed height (amount of adsorbent) on the breakthrough curve

The dynamic adsorption of MB is largely dependent on the bed height, which is directly proportional to the quantity of GS in the column (Kanadasan *et al.* 2010). To produce 5, 10 and 15 cm of bed height, 5, 10 and 15 g of GS were used, respectively. The breakthrough capacity ($q_{50\%}$) increased from 0.181 to 0.296 $mg.g^{-1}$ when the bed height (adsorbent mass) increased from 5 to 15 cm, this is due to an increase in the surface area of the adsorbent, which provided more activated sites for MB binding (Zulfadhly *et al.* 2001). At the same time, the higher bed column resulted in a decrease in the solute concentration in the aqueous solution (Han *et al.* 2009). Breakthrough time, exhaustion time and the volume of treated solution also increase with the bed height. These results were in agreement with those reported in previous studies (Al-Degs *et al.* 2009).

Effect of initial concentration on the breakthrough curve

The effect of different initial MB concentrations (5, 10 and 15 $mg.L^{-1}$) on the adsorption process was investigated. It can be deduced that a slower breakthrough curve will be obtained at a lower initial concentration. This may be explained by the fact that a lower concentration gradient caused slower transport due to a decreased diffusion or mass transfer coefficient (Uddin *et al.* 2009; Lezehari *et al.* 2012; Sadaf & Bhatti 2014). Higher initial concentrations led to a higher driving force for mass transfer, hence the adsorbent saturation was achieved more quickly, which resulted in a decrease in the breakthrough and exhaustion time and adsorption zone length (Malkoc *et al.* 2006; Baral *et al.* 2009).

Effect of flow rate on the breakthrough curve

In order to perform this investigation, the effect of different flow rates (1, 2 and 3 $mL{\cdot}min^{-1}$) was studied. From Table 3 it can be seen that the breakthrough time decreases as the flow rate increases. The faster breakthrough point at higher flow rates is due to reduced contact time between dye molecules and adsorbent (Sadaf & Bhatti 2014). Therefore, the MB solution will leave the bed before the equilibrium can be reached, which will result in a decreasing amount of MB

Table 2 | Chemical composition of GS of Arcelor-Mittal (Algeria)

Constituents	SiO_2	CaO	Al_2O_3	MgO	Fe_2O_3	TiO_2	MnO	S	K_2O	Na_2O	BaO
(massic %)	35.68	42.17	7.92	7.49	0.5	0.29	3.04	1.518	0.51	0.29	1.74

Table 3 | Column data and parameters with different conditions

Initial concentration C_0 (mg.L^{-1})	Bed height Z (cm)	Flow rate Q (mL.min^{-1})	Breakthrough time t_b (min)	Exhaustion time t_e (min)	Breakthrough capacity $q_{,exp\ (50\%)}$ (mg.g^{-1})
5	10	2	134	282.97	0.19
10	10	2	91.17	260.21	0.23
15	10	2	39.15	165.64	0.16
10	5	2	31.17	196.67	0.18
10	15	2	158.55	292.42	0.29
10	10	3	40.33	236.57	0.19
10	10	1	145.91	309.93	0.22

being adsorbed. (Kanadasan *et al.* 2010). This result was in agreement with the findings of other researchers in the literature (Taty-Costodes *et al.* 2005; Li *et al.* 2011).

The adsorption capacity of the GS was found to be lower than that of many other adsorbents (Han *et al.* 2007; Zhang *et al.* 2011; Tarawou *et al.* 2014); the main reason could be the poor porosity and low surface area of the adsorbent (Grassi *et al.* 2012).

The pH values of influent and effluent during adsorption

The breakthrough curve with various influent pH (3, 5, 7.5, 9 and 12) is shown in Figure 2. The appropriate pH was adjusted by adding 0.1 M NaOH or HCl.

As shown in Figure 2, it may be noted that pH 3 and 12 did not promote the adsorption of MB onto GS. Our adsorbent consists essentially of silicates and aluminosilicates of calcium. As in Runzhang *et al.* (1988), the highly acidic and alkalic influents provoke the solubilization of these constituents and therefore the destruction of the structure of our GS, which results in a clogging of the column. On the other hand, it is obvious that pH 7.5 is the most appropriate for obtaining a higher breakthrough time and thus a higher adsorption capacity of MB.

Figure 3 shows the effluent pH values after adsorption for different influents.

It can be observed that there is always an increase in effluent pH values during adsorption.

Breakthrough curve assessment

For the Bohart–Adams model, the characteristic parameters such as N_o and K_{BA} can be calculated from the linear plot of ln (C_t/C_0) against t (Equation (1)) at different bed heights,

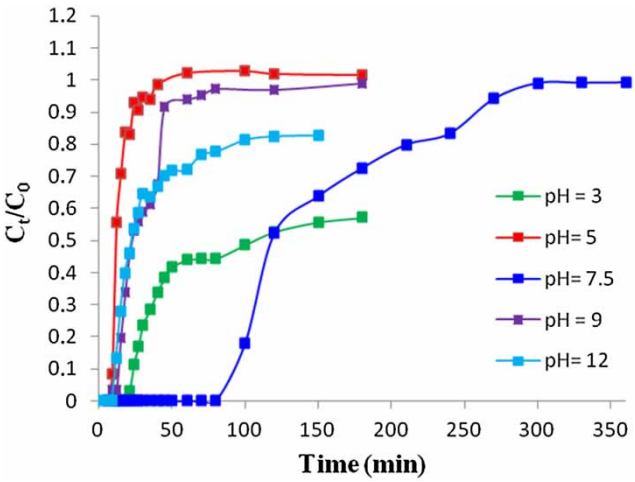

Figure 2 | Breakthrough curves for adsorption of MB on GS at different influent pH (Z = 10 cm, C_0 = 10 mg.L^{-1}, Q = 2 mL.min^{-1}).

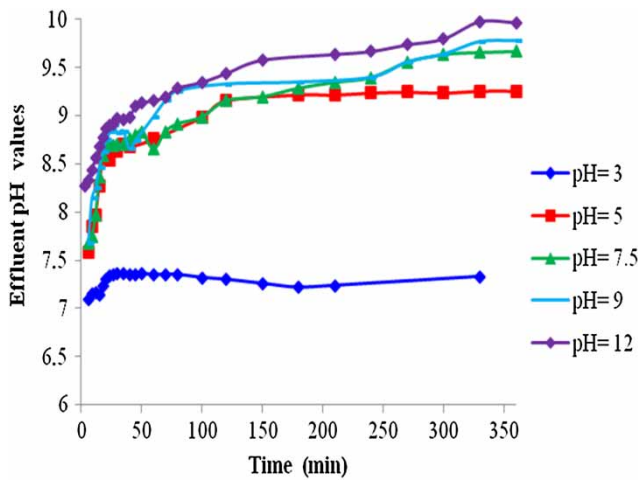

Figure 3 | The effluent pH values after adsorption of MB by GS.

concentrations and flow rates. The obtained results are represented in Table 4 and Figure 4, where there is an increase in the initial concentration from 5 to 15 mg.L^{-1}, the saturation concentration of MB increases from 259.5 to 294.4 mg.L^{-1}. On the other hand, with increasing flow rate the saturation concentration of MB decreased. The R^2 values vary between 0.64 and 0.98. Nevertheless, most of the R^2 values are superior to 0.9 and *SS* values range between 0.001 and 0.135), which indicates that the data fits into the model perfectly (Kanadasan *et al.* 2010).

Table 4 | Bohart–Adams model parameters at various conditions

C_0 (mg.L^{-1})	Z (cm)	Q (mL.min^{-1})	k_{BA} (L.mg^{-1}.min^{-1}) $\times 10^3$	N_o (mg.L^{-1})	R^2	SS
5	10	2	2.94	259.5	0.89	0.008
10	10	2	5.91	274.68	0.98	0.001
15	10	2	1.76	294.4	0.64	0.034
10	5	2	131.2	212.8	0.93	0.038
10	15	2	0.85	430.5	0.99	0.018
10	10	1	1.77	558.3	0.93	0.002
10	10	3	12.68	215.9	0.76	0.135

For the BDST model, a plot of t versus Z (Equation (2)) is expected to yield a linear curve, in which N_o' and K_a could be evaluated from the slope and y-axis intersection point, respectively. The results are listed in Table 5 and shown in Figure 5.

From these results it can be deduced that at different C_t/C_0 ratios, the values of the correlation coefficient are high, which show good agreement of the experimental data with the BDST model.

For the Thomas model, maximum adsorption capacity of the adsorbent (q,cal) and kinetic constant (k_{TH}) are determined by fitting the experimental data into Equation (3). Linear regression results, with correlation coefficients and *SS* values, are listed in Table 6 and presented in Figure 6. It can be observed that for a given experimental condition, the experimental and calculated values are similar. Also, most of the R^2 values were greater than 0.89 with smaller *SS* (less than 0.016), which validates the use of the

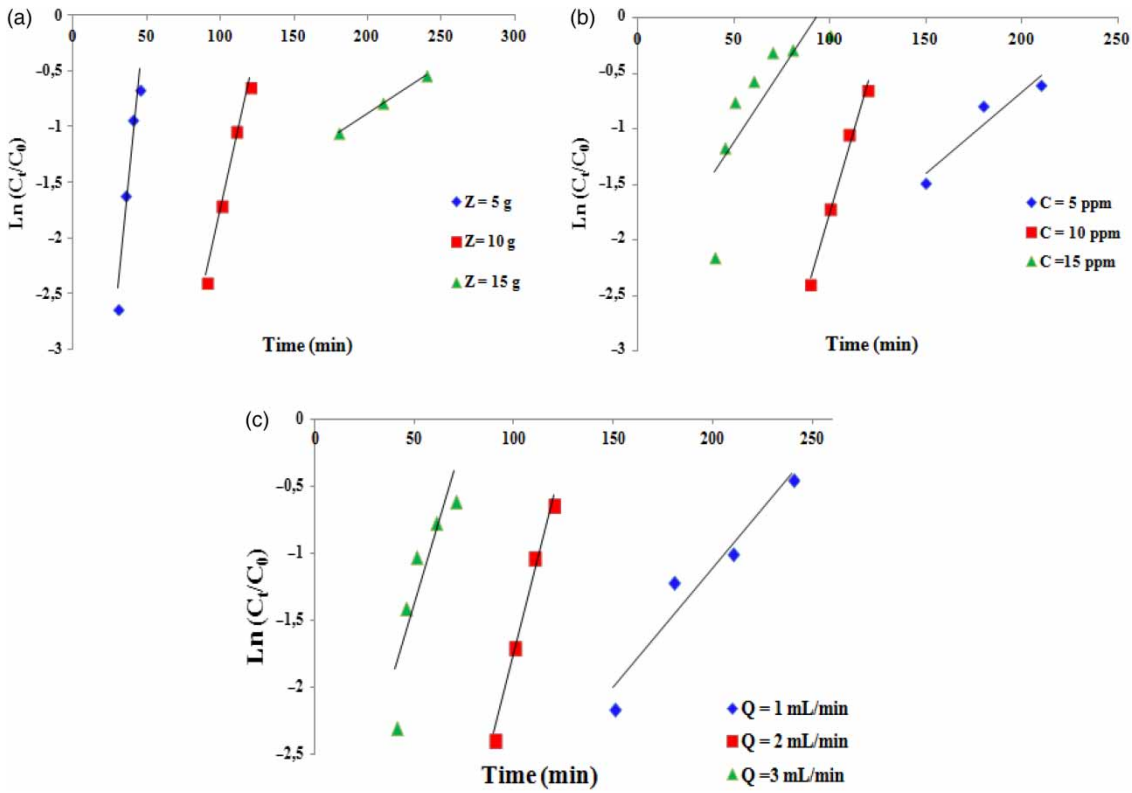

Figure 4 | Linear regression of Bohart–Adams model with experimental data at different conditions: (a) Z, (b) C_0 and (c) Q.

Table 5 | Bed depth service time of column at different bed height ($C = 10$ mg.L^{-1} and $Q = 0.9$ mL.min^{-1})

C_t/C_0	K_a (L.mg^{-1}.min^{-1})	N_0' (mg.L^{-1})	R^2
10%	−0.0065	269.24	0.99
90%	−0.0014	209.88	0.96

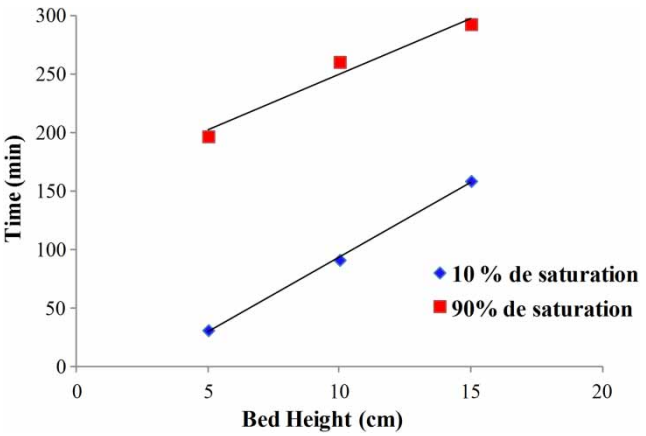

Figure 5 | Linear regression of the BDST model at different breakthrough points with C_0=10 mg.L^{-1} and $Q = 2$ mL.min^{-1}.

Table 6 | Thomas model parameters at various conditions

C_0 (mg.L^{-1})	Z (cm)	Q (mL. min^{-1})	K_{TH} (L.mg^{-1}.min^{-1}) ×10^{2}	$q_{,cal}$ (mg.g^{-1})	R^2	$q_{,exp}$ (mg.g^{-1})	SS
5	10	2	0.60	0.199	0.90	0.195	0.004
10	10	2	0.20	0.280	0.89	0.236	0.012
15	10	2	0.17	0.181	0.74	0.160	0.014
10	5	2	0.20	0.248	0.71	0.181	0.016
10	15	2	0.28	0.285	0.90	0.296	0.003
10	10	1	0.27	0.223	0.98	0.191	0.001
10	10	3	0.16	0.274	0.83	0.224	0.008

Thomas model to predict the maximum adsorption capacity of the bed (Kanadasan *et al.* 2010).

Comparison of Bohart–Adams and Thomas models

According to the values of R^2 and *SS* listed in Tables 4 and 6 at the same experimental conditions, the values of R^2 from Bohart–Adams (0.64–0.98) were larger than those from the Thomas model (0.71–0.98). Comparing the *SS* values, we notice that the *SS* values of the Thomas model are higher than those of the Bohart–Adams only when $C_0 = 10$ mg.L^{-1}, $Z = 10$ cm, $Q = 2$ mL.min^{-1}. These results showed that both models can be selected to predict the column process of MB onto GS.

Column regeneration

The column with a bed depth of 10 cm and flow rate of 2 mL.min^{-1} saturated with 10 mg.L^{-1} of MB was selected for a desorption study. Desorption was carried out, and deionized water was used as the desorbing agent. The concentration of MB was measured at different time intervals as shown in Figure 7.

It was observed that the desorption cycle took 50 min, after which further desorption was negligible.

Reuse study of regenerated column

To check the adsorption efficiency of the regenerated GS column, it was reloaded with a dye solution of 10 mg.L^{-1} at a rate of 2 mL.min^{-1}.

The breakthrough curve obtained was compared with that of GS (10 cm depth; 10 mg.L^{-1} MB concentration, flow rate of 2 mL.min^{-1}), and is shown in Figure 8.

For GS, the breakthrough time was 91.17 min and exhaustion time was 260.21 min. However, it was decreased for regenerated GS (breakthrough time was 14.30 min and exhaustion time was 249.46 min).

CONCLUSIONS

In the present study, the GS packed bed was used to analyze the column dynamics in the adsorption process. The effect of bed height, initial MB concentration and flow rate on breakthrough curves has been investigated. A higher uptake of MB was observed at higher bed depth ($Z =$ 15 cm). Both breakthrough time and exhaustion time increased with increasing bed height, but decreased with increasing MB initial concentration. Besides, a faster breakthrough curve has been found at higher flow rates. According to the obtained results, the granulated slag can

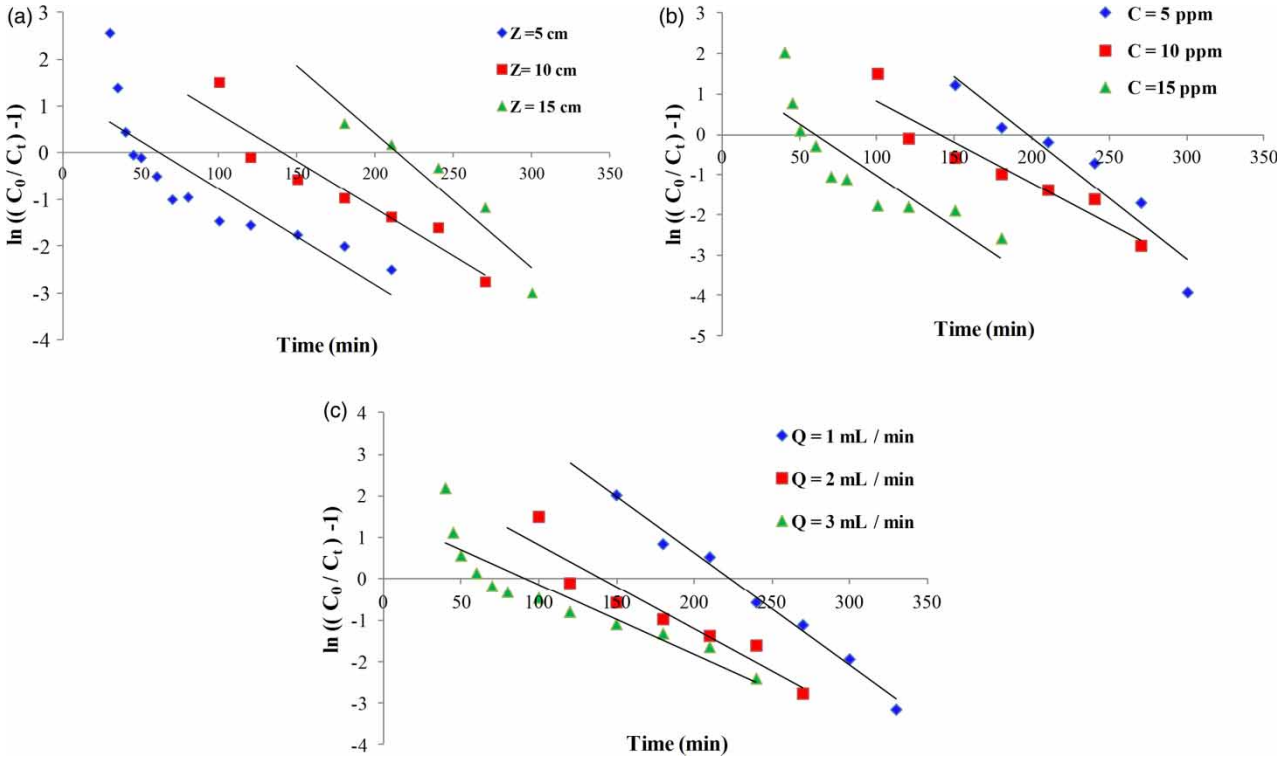

Figure 6 | Linear regression of the Thomas model with experimental data at different conditions: (a) Z, (b) C_0 and (c) Q.

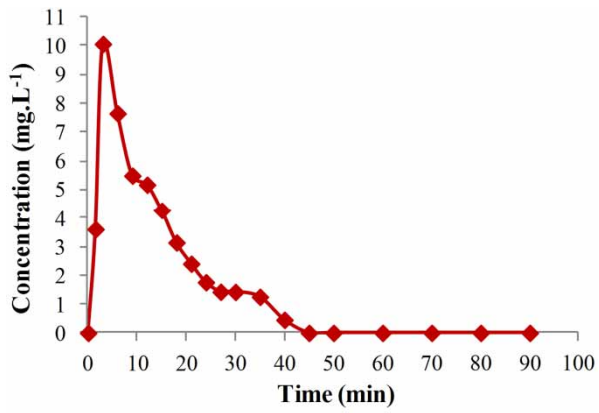

Figure 7 | First cycle desorption profile of MB.

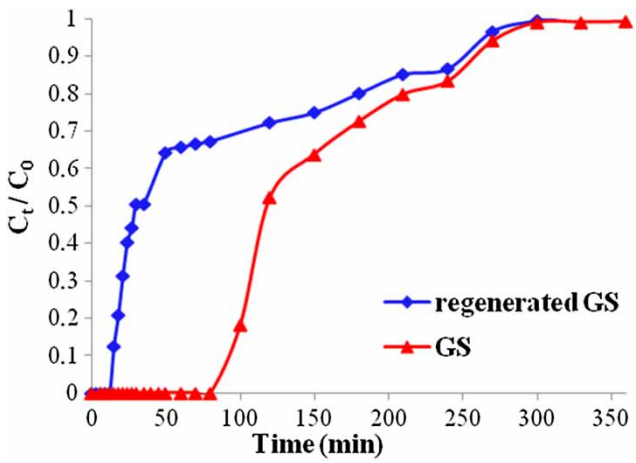

Figure 8 | Comparative breakthrough curve for original and regenerated GS.

be proposed as an adsorbent in the treatment of wastewater for the removal of dye from an aqueous solution. The dynamic behavior of the column was predicted by the Bohart–Adams, BDST, and Thomas models. All models were found suitable for describing the whole or a definite part of the dynamic behavior of the column.

REFERENCES

Abdul Halim, H. N. & Kar Mee, K. L. 2011 Adsorption of basic Red 46 by granular activated carbon in a fixed bed column. *Int. Conf. Environ. Indust. Innov.* **12**, 263–267.

Ader, R. 1981 *Psychoneuroimmunology*. Academic Press, New York, 321 pp.

Ahmad, A. A. & Hameed, B. H. 2010 Fixed-bed adsorption of reactive azo dye onto granular activated carbon prepared from waste. *J. Hazard. Mater.* **175**, 298–303.

Aksu, Z. 2005 Application of biosorption for the removal of organic pollutants: a review. *Process. Biochem.* **40**, 997–1026.

Al-Degs, Y. S., Khraisheh, M. A. M., Allen, S. J. & Ahmad, M. N. 2009 Adsorption characteristics of reactive dyes in columns of activated carbon. *J. Hazard. Mater.* **165**, 944–949.

Arabi, N., Jauberthie, R. & Sellami, A. 2012 Briques silico-calcaires autoclavées: influence de l'addition de laitier de haut fourneau sur la formation des phases. *Mater. Struct.* **46** (1–2), 181–190.

Atshan, A. A. 2014 Adsorption of methyl green dye onto bamboo in batch and continuous system. *Iraq J. Chem. Pet. Eng.* **15** (1), 65–72.

Baral, S. S., Das, N., Ramulu, T. S., Sahoo, S. K., Das, S. N. & Chaudhury, G. R. 2009 Removal of Cr(VI) by thermally activated weed Salvinia cucullata in a fixed-bed column. *J. Hazard. Mater.* **161**, 1427–1435.

Blackburn, R. S. 2004 Natural polysaccharides and their interactions with dye molecules: applications in effluent treatment. *Environ. Sci. Technol.* **38**, 4905–4909.

Bohart, G. S. & Adams, E. Q. 1920 Some aspects of the behaviour of the charcoal with respect chlorine. *J. Am. Chem. Soc.* **42**, 523–544.

Brunauer, S., Emmett, P. H. & Teller, E. 1938 Adsorption of gases in multimolecular layers. *J. Am. Chem. Soc.* **60**, 309–319.

Cheknane, B., Badu, M., Basly, J. P., Bouras, O. & Zermane, F. 2012 Modeling of basic green 4 dynamic sorption onto granular organo–inorgano pillared clays (GOICs) in column reactor. *Chem. Eng. J.* **209**, 7–12.

Crini, G. 2006 Non-conventional low-cost adsorbents for dye removal: a review. *Bioresour. Technol.* **97**, 1061–1085.

Das, B., Prakash, S., Reddy, P. S. R. & Misra, V. N. 2007 An overview of utilization of slag and sludge from steel industries. *Resour. Conserv. Recycl.* **50**, 40–57.

Dimitrova, S. V. & Mehandgiev, D. R. 1998 Lead removal from aqueous solution by granulated blast-furnace slag. *Water Res.* **32**, 3289–3292.

Elkassimi, M., Meziane, D., Abouarnadasse, S. & Azizi, H. 1998 Elimination des colorants de l'industrie de textile par le charbon de bois. *2ème Conférence Maghrébine de Génie des Procédés*, Gabès (Tunisie), ENIG.

Faust, S. D. & Aly, O. M. 1987 *Adsorption Processes for Water Treatment*. Butterworth Publishers, Boston.

Fewson, C. A. 1998 Biodegradation of xenobiotic and other persistent compounds: the causes of recalcitrance. *Trends Biotechnol.* **6**, 148–153.

Grassi, M., Kaykioglu, G., Belgiorno, V. & Lofrano, G. 2012 Emerging compounds removal from wastewater. *Springer Briefs Green Chem. Sustain.* **10** (1007), 978–994.

Han, R. P., Wang, Y., Zou, W., Wang, Y. F. & Shi, J. 2007 Comparison of linear and nonlinear analysis in estimating the Thomas model parameters for methylene blue adsorption onto natural zeolite in fixed-bed column. *J. Hazard. Mater.* **145**, 331–335.

Han, R. P., Wang, Y., Zhao, X., Wang, Y. F., Xie, F. L., Cheng, J. M. & Tang, M. S. 2009 Adsorption of methylene blue by phoenix tree leaf powder in a fixed-bed column: experiments and prediction of breakthrough curves. *Desalination* **245**, 284–297.

Hutchins, R. A. 1973 New method simplifies design of activated carbon systems. *Chem. Eng.* **80**, 133–138.

Janet, A., Kumaresan, R. & Uma Maheshwari, S. 2015 Removal of dyes in adsorption column. *J. Chem. Pharm. Res.* **7** (3), 1718–1723.

Kanadasan, G., Mashitah, M. D. & Vadivelu, V. M. 2010 Fixed bed adsorption of methylene blue by using palm oil mill effluent waste activated sludge. In: *3rd ISWA Asia Pacific Young Water Professional Conference 2010 Achieving Sustainable Development in the New Era*, Singapore.

Kostura, B., Kulveitova, H. & Lesko, J. 2005 Blast furnace slags as sorbents of phosphate from water solutions. *Water Res.* **39**, 1795–1802.

Kumar, M. & Tamilarasan, R. 2013 Modeling of experimental data for the adsorption of methyl orange from aqueous solution using a low cost activated carbon prepared from Prosopis julifl ora. *Pol. J. Chem. Technol.* **15** (2), 29–39.

Lezehari, M., Baudu, M., Bouras, O. & Basly, J. P. 2012 Fixed-bed column studies of pentachlorophenol removal by use of alginate encapsulated pillared clay microbeads. *J. Colloid Interface Sci.* **379** (1), 101–106.

Li, L., Dai, W., Yu, P., Zhao, J. & Qu, Y. 2009 Decolorisation of synthetic dyes by crude laccase from *Rigidoporus lignosus* W1. *J. Chem. Tech. Biotechnol.* **84** (3), 399–404.

Li, W., Yue, Q., Tu, P., Ma, Z., Gao, B., Li, J. & Xu, X. 2011 Adsorption characteristics of dyes in columns of activated carbon prepared from paper mill sewage sludge. *Chem. Eng. J.* **178**, 197–203.

Malkoc, E., Nuhoglu, Y. & Dundar, M. 2006 Adsorption of chromium(VI) on pomace – an olive oil industry waste: batch and column studies. *J. Hazard. Mater.* **138**, 142–151.

Mathialagan, T. & Viraraghavan, T. 2002 Adsorption of cadmium from aqueous solution by perlite. *J. Hazard. Mater.* **B94**, 291–303.

Milenova, K. I., Nikolov, P. M., Georgieva, A. L., Batakliev, T. T., Georgiev, V. F. & Rakovsky, S. K. 2014 Discoloration of reactive dyes in wastewaters by ozonation. *J. Int. Sci. Publ. Ecol. Saf.* **8**, 1314–7234.

Mustafa, A. I., Alam, S., Amin, N., Bahadur, N. M. & Habib, A. 2008 Phenol removal from aqueous system by jute stick. *Pak. J. Anal. Environ. Chem.* **9**, 92–95.

Pearce, C. I., Lloyd, J. R. & Guthrie, J. T. 2003 The removal of colour from textiles wastewater using whole bacterial cells: a review. *Dyes Pigments* **58**, 179–196.

Ramakrishna, K. R. & Viraraghvan, T. 1997 Use of slag for dye removal. *Waste Manage.* **17** (8), 483–488.

Runzhang, Y., Qiongying, G. & Shixi, O. 1988 Study on structure and latent hydraulic activity of slag and its activation mechanism. *Silicates Indust.* **53** (3–4), 55–59.

Sadaf, S. & Bhatti, H. N. 2014 Batch and fixed bed column studies for the removal of Indosol Yellow BG dye by peanut husk. *J. Taiwan Inst. Chem. Eng.* **45**, 541–553.

Sampedro, I., Romero, C., Ocampo, J. A., Brenes, M. & Habib, A. 2004 Removal of monomeric phenols in dry mill olive residue by saprobic fungi. *J. Agr. Food. Chem.* **52**, 4487–4492.

Seshadri, S., Bishop, P. L. & Agha, A. M. 1994 Anaerobic/aerobic treatment of selected azo dyes in wastewater. *Waste Manage.* **15**, 127–137.

Suksabye, P., Thiravetyan, P. & Nakbanpote, W. 2008 Column study of chromium (VI) adsorption from electroplating industry by coconut coir pith. *J. Hazard. Mater.* **160**, 56–62.

Tan, I. A. W., Hameed, B. H. & Ahmad, A. L. 2007 Equilibrium and kinetic studies on basic dye adsorption by oil palm fibre activated carbon. *Chem. Eng. J.* **127**, 111–119.

Tarawou, T., Young, E. & Ere, D. 2014 Adsorption of methylene blue dye from aqueous solution using activated carbon produced from water hyacinth in a fixed–bed column system. *Sch. Acad. J. Biosci.* **2** (9), 607–612.

Taty-Costodes, V. C., Fauduet, H., Porte, C. & Ho, Y. S. 2005 Removal of lead (II) ions from synthetic and real effluents using immobilized Pinus svlvestris sawdust: adsorption on a fixed column. *J. Hazard. Mater.* **123**, 135–144.

Thomas, H. C. 1944 Heterogeneous ion exchange in flowing system. *J. Am. Chem. Soc.* **66**, 1664–1666.

Uddin, M. T., Rukanuzzaman, M., Rahman Khan, M. M. & Islam, M. A. 2009 Adsorption of methylene blue from aqueuse solution by jackfruit (Artocarpus heteropyllus) leaf powder: a fixed- bed column study. *J. Environ. Manage.* **90**, 3443–3450.

Zhang, W., Dong, L., Yan, H., Li, H., Jiang, Z., Kan, X., Yang, H., Li, A. & Cheng, R. 2011 Removal of methylene blue from aqueous solutions by straw based adsorbent in a fixed-bed column. *Chem. Eng. J.* **173**, 429–436.

Zhou, Y. F. & Haynes, R. J. 2010 Sorption of heavy metals by inorganic and organic components of solid wastes: significance to use of wastes as low-cost adsorbents and immobilizing agents. *Water Air Soil Pollut.* **215**, 631–643.

Zulfadhly, Z., Mashitah, M. D. & Bhatia, S. 2001 Heavy metals removal in fixed-bed column by the macro fungus Pycnoporus sanguineus. *Environ. Pollut.* **112**, 463–470.

Zulfikar, M. A. & Setiyanto, H. 2013 Adsorption of congo red from aqueous solution using powdered eggshell. *Int. J. Chem. Tech. Res.* **5** (4), 1532–1540.

First received 26 April 2015; accepted in revised form 4 August 2015. Available online 14 September 2015